



Published in final edited form as:

Clin Cancer Res. 2011 June 1; 17(11): 3551–3557. doi:10.1158/1078-0432.CCR-10-3087.

Detection of tumor DNA at the margins of colorectal cancer liver metastasis

Matthias Holdhoff^{1,*}, Kerstin Schmidt^{1,*}, Frank Diehl⁴, Nishant Aggrawal¹, Philipp Angenendt⁴, Katharine Romans¹, Daniel L. Edelstein¹, Michael Torbenson², Kenneth W. Kinzler¹, Bert Vogelstein¹, Michael A. Choti^{3,†}, and Luis A. Diaz Jr^{1,5,†}

¹Ludwig Center for Cancer Genetics and Therapeutics and Howard Hughes Medical Institute at Johns Hopkins Kimmel Cancer Center, Baltimore, MD 21231, USA

²The Department of Pathology, Johns Hopkins Medical Institutes, Baltimore, MD 21231, USA

³The Department of Surgery, Johns Hopkins Medical Institutes, Baltimore, MD 21231, USA

⁴Inostics GmbH, Hamburg, Germany

⁵Swim Across America Laboratory at Johns Hopkins, Baltimore, MD 21231

Abstract

Purpose—Defining an adequate resection margin of colorectal cancer liver metastases is essential for optimizing surgical technique. We have attempted to evaluate the resection margin through a combination of histopathologic and genetic analyses.

Experimental Design—We evaluated 88 samples of tumor margins from 12 patients with metastatic colon cancer who each underwent partial hepatectomy of one to six liver metastases. Punch biopsies of surrounding liver tissue were obtained at 4, 8, 12 and 16 mm from the tumor border. DNA from these biopsies was analyzed by a sensitive PCR-based technique, called BEAMing, for mutations of KRAS, PIK3CA, APC, or TP53 identified in the corresponding tumor.

Results—Mutations were identified in each patient's resected tumor and used to analyze the 88 samples circumscribing the tumor-normal border. Tumor-specific mutant DNA was detectable in surrounding liver tissue in five of these 88 samples, all within 4 mm of the tumor border. Biopsies that were 8, 12, and 16 mm from the macroscopic visible margin were devoid of detectable mutant tumor DNA as well as of microscopically visible cancer cells. Tumors with a significant radiologic response to chemotherapy were not associated with any increase in mutant tumor DNA in beyond 4 mm of the main tumor.

Conclusions—Mutant tumor-specific DNA can be detected beyond the visible tumor margin, but never beyond 4 mm, even in patients whose tumors were larger prior to chemotherapy. These data provide a rational basis for determining the extent of surgical excision required in patients undergoing resection of liver metastases.

Introduction

Margin status is one of the most important factors in determining the success of a solid tumor resection. Surgical margins that show the presence of cancer cells have an increased

[†]To whom correspondence should be addressed to Luis Diaz (ldiaz1@jhmi.edu) or Michael Choti (mchoti1@jhmi.edu).

*These authors contributed equally to this work.

Parts of this work were presented at the 2010 Annual Meeting of the American Society of Clinical Oncology.

risk of local recurrence, aggressive biology and a decreased overall survival (1–4). As a result, a margin of normal tissue surrounding the perimeter of the resected tumor is always included as part of the resected tumor specimen when possible. Historically, a circumferential rim of at least 1 cm around the macroscopically visible metastatic lesion is removed. While more recently, the width of surgical margin has been challenged, achievement of negative margins remains important in order to optimize long-term outcome in these patients (3).

Despite gross and microscopic review of the margins of a surgical resection, some patients will have local recurrence of their tumors at the site of surgery, thereby suggesting that standard microscopic evaluation of the surgical margins may not be sufficient in many cases (2). Moreover, the extent of the necessary surgical margin in patients following response to preoperative chemotherapy is less clear.

An analytic approach could provide evidence that would help determine the width of the surgical margin required in resection of hepatic colorectal metastases, whether untreated or following response to preoperative chemotherapy. Careful histopathologic assessment can in principle be used for assessing the presence of tumor cells outside the tumor-liver border. However, histopathologic analysis can miss small numbers of cancer cells. We therefore supplemented histopathologic analysis with a molecular genetic approach, using patient-specific somatic mutations as exquisitely specific indicators of the presence of tumor cells in clinical samples.

Traditional mutation detection methods cannot readily detect mutations when they are present at less than 1% of the DNA templates under study. This fraction of tumor involvement in a sample would be visible by microscopy and we were interested in detecting smaller quantities of tumor cells. We therefore turned to a highly sensitive digital PCR-based assay, termed BEAMing (5), for this study. The method is named after its components (Beads, Emulsification, Amplification and Magnetics) and can detect mutations in samples that contain as few as 1 in 100,000 mutant DNA fragments (6). In this study, we applied this approach to evaluate the ostensibly normal liver closely circumscribing surgically resected metastatic lesions.

Materials and Methods

Patient Selection

Patients with colorectal cancer undergoing planned resection of liver metastases and who underwent partial hepatectomy were eligible for this study. Those patients with multiple tumors undergoing major hepatic resection with >1-cm resection margins were included in order to optimize the analysis, including chemo-naïve, chemo-responders, and non-responders. The study was approved by the Johns Hopkins Institutional Review Board and written consent was obtained from all patients prior to their enrollment in the protocol.

Sample collection

Freshly resected liver tissue was cut into 0.5 – 1.0 cm slices and processed immediately following surgical resection. Punch biopsies of 4 mm in diameter were obtained radially from surrounding liver tissue at 4, 8, 12 and 16 mm distances from the macroscopically visible tumor border. The number of biopsies in each direction (away from the macroscopically visible tumor border) varied between 1 and 4, depending on the individual geometry of each tissue specimen (see Supplementary Figure 1). The samples were immediately cryopreserved and the ends of the punch biopsies were preserved in formalin. One punch biopsy was taken from the tumor itself for mutation analysis and one sample was obtained from normal liver tissue far removed from any metastasis as a negative control.

DNA Purification of Frozen Tumor Tissue

Frozen tumor tissue sections were mounted on slides and microdissected with the PALM microscope. The dissected tissue was digested overnight at 60°C in 15 µl ATL buffer (Qiagen, Hilden, Germany) and 10 µl Proteinase K (20 mg/ml; Invitrogen, Carlsbad, CA). DNA was isolated using the QIAamp DNA Micro Kit (Qiagen, Hilden, Germany) following the manufacturer's protocol.

DNA Purification of Frozen Liver Tissue

Frozen punch biopsies (~ 50 mg) were mixed with 1 ml of Cell Lysis Solution CLS-TC and homogenized in the FASTPrep (Q Biogene, Inc.) instrument for 40 seconds at a speed setting of 6.0. Tissue debris was removed by centrifugation and the supernatant was transferred to a new microcentrifuge tube. Binding, washing and elution steps were performed according to the FASTPrep protocol supplied by the manufacturer.

DNA Quantification

DNA isolated from tissue samples was quantified using a modified version of a human LINE-1 real-time PCR assay (7). The primer set was designed to amplify the most abundant consensus region of the human LINE-1 family (amplicon 97 bp; forward primer TGGCACATATACACCATGGAA; reverse primer TGAGAATGATGGTTTCCAATTC). PCR was performed in a 25 µl reaction volume consisting of 4 µl of various dilutions of template DNA, 0.5 U of Platinum Taq DNA Polymerase, 1× PCR buffer, 6% (v/v) DMSO, 1 mM of each dNTP, 1:100,000 dilution of SYBR Green I (Invitrogen, Carlsbad, CA), and 0.2 µM of each primer. Amplification was carried out in an iCycler (Bio-Rad) using the following cycling conditions: 94°C for 1 min; 3 cycles of 94°C for 30 s, 67°C for 30 s, 70°C for 1 min; 3 cycles of 94°C for 30 s, 64°C for 35 s, 70°C for 1 min, 3 cycles of 94°C for 30 s, 61°C for 30 s, 70°C for 1 min; 35 cycles of 94°C for 30 s, 59°C for 30 s, 70°C for 1 min. Various dilutions of normal human lymphocyte DNA were incorporated in each plate setup to serve as standards. The threshold cycle number was determined using Bio-Rad analysis software with the PCR baseline subtracted.

Sequencing of Tissue DNA for Mutations

All DNA samples isolated from tumor tissue were analyzed for mutations in 26 regions of *APC*, one region of *KRAS*, two regions of *PIK3CA*, and four regions of *TP53* using direct Sanger sequencing. The first PCR was performed in a 10 µl reaction volume containing 50–100 genome equivalents (GEs) of template DNA (1 GE equals 3.3 pg of human genomic DNA), 0.5 U of Platinum Taq DNA Polymerase (Invitrogen, Carlsbad, CA), 1× PCR buffer (67 mM of Tris-HCl, pH 8.8, 67 mM of MgCl₂, 16.6 mM of (NH₄)₂SO₄, and 10 mM of 2-mercaptoethanol), 2 mM ATP, 6% (v/v) DMSO, 1 mM of each dNTP, and 0.2 µM of each primer. The sequences of the primer sets were described previously in Diehl et al (8). The amplification was carried out under the following conditions: 94°C for 2 min; 3 cycles of 94°C for 15 s, 68°C for 30 s, 70°C for 15 s; 3 cycles of 94°C for 15 s, 65°C for 30 s, 70°C for 15 s, 3 cycles of 94°C for 15 s, 62°C for 30 s, 70°C for 15 s; 40 cycles of 94°C for 15 s, 59°C for 30 s, 70°C for 15 s. One microliter of the first amplification was then added to a second 10-µl PCR reaction mixture of the same makeup as the one described above, except that different primers were used. The second (nested) PCR reaction was temperature-cycled using the following conditions: 2 min at 94°C; 15 cycles of 94°C for 15 s, 58°C for 30 s, 70°C for 15 s. The PCR products were purified and sequenced as described in Jones et al(9) with primers containing a 30 bp polyT tag attached to the 5' prime end to improve the sequence quality for the first 30 bases (Tag1 primer: 5'-(dT)₃₀-tcccgcgaattaatacagac; M13 primer: 5'-(dT)₃₀-gtaaacgacggccagt). Data analysis was performed using Mutation Explorer (SoftGenetics, State College, PA).

BEAMing of Tumor Margin DNA for Mutations

150,000 GE were used for each BEAMing assay. An initial amplification with a high fidelity DNA polymerase was performed in five separate 50 μ l PCR reactions each containing template DNA, 5 \times Phusion High Fidelity PCR buffer (NEB), 1.5 U of Hotstart Phusion polymerase (NEB), 0.2 μ M of each primer, 0.25 mM of each dNTP, and 0.5 mM MgCl₂. Pre-amplification primers and temperature cycling conditions are listed in Supplementary Table 1, a second PCR nested) was performed by adding 2 μ l of the first amplification to a 20- μ l PCR reaction of the same makeup as the first one for selected mutations. PCR products were pooled, diluted, and quantified using the PicoGreen dsDNA assay (Invitrogen, Carlsbad, CA). The fluorescence intensity was measured using a CytoFluor multiwell plate reader (PE Biosystems) and the DNA quantity was calculated using Lambda-phage DNA reference standards.

Emulsion PCR was performed as described previously (3). Briefly, a 150 μ l PCR mixture was prepared containing 20 pg template DNA, 42.5 U of Platinum Taq DNA polymerase (Invitrogen, Carlsbad, CA), 1 \times PCR buffer (see above), 0.2 mM dNTPs, 5 mM MgCl₂, 0.05 μ M Tag1 (5'-tcccgcgaaattaatcagac-3'), 8 μ M Tag2 (5'-gctggagctctcagcta-3') and $\sim 6 \times 10^7$ magnetic streptavidin beads (MyOne, Invitrogen, Carlsbad, CA) coated with Tag1 oligonucleotide (5'-dual biotin-T-Spacer18- tcccgcgaaattaatcagac-3'). The 150 μ l PCR reaction, 600 μ l oil/emulsifier mix (7% ABIL WE09, 20% mineral oil, 73% Tegosoft DEC, Evonik Goldschmidt Cooperation, Hopewell, VA), and one 5 mm steel bead (Qiagen, Hilden, Germany) were added to a 96 deep well plate 1.2 ml (Abgene, Epsom, UK). Emulsions were prepared by shaking the plate in a TissueLyser (Qiagen, Hilden, Germany) for 10 s at 15 Hz and then 7 s at 17 Hz.

Emulsions were dispensed into eight PCR wells and temperature cycled at 94°C for 2 min; 3 cycles of 94°C for 10 s, 68°C for 45 s, 70°C for 75 s; 3 cycles of 94°C for 10 s, 65°C for 45 s, 70°C for 75 s, 3 cycles of 94°C for 10 s, 62°C for 45 s, 70°C for 75 s; 50 cycles of 94°C for 10 s, 59°C for 45 s, 70°C for 75 s.

To break the emulsions, 150 μ l breaking buffer (10 mM Tris-HCl, pH 7.5, 1% Triton-X 100, 1% SDS, 100 mM NaCl, 1 mM EDTA) was added to each well and mixed with a TissueLyser at 20 Hz for 20 s. Beads were recovered by centrifuging the suspension at 3,200 g for 2 min and by removing the oil phase. This breaking step was repeated twice. All beads from 8 wells were consolidated and washed with 150 μ l wash buffer (20 mM Tris-HCl, pH 8.4, 50 mM KCl). The DNA on the beads was denatured for 5 min with 0.1 M NaOH. Finally, beads were washed with 150 μ l wash buffer and resuspended in 150 μ l of the same buffer. The mutation status of DNA bound to beads was determined by allele-specific hybridization. Fluorescently labeled probes complementary to the mutant and wild-type DNA sequences, designed for the different mutations were used. The size of the probes ranged from 15 to 18 nt, depending on the GC content of the target region. All mutant probes were coupled to a Cy5TM fluorophore and all wild-type probes were coupled to a Cy3TM fluorophore at their 5' ends (Integrated DNA Technologies or Biomers). In addition, oligonucleotides that bound to a separate location within the amplicon ("universal probes") were used to label every extended PCR product as a positive control. These amplicon-specific probes were synthesized with a ROXTM fluorophore attached to their 5' ends. Probe sequences are listed in Supplementary Table 2. Each allele-specific hybridization reaction contained $\sim 1 \times 10^7$ beads in 30 μ l wash buffer (see above), 66 μ l of 1.5 \times hybridization buffer (1.5 \times = 4.5 M tetramethylammonium chloride, 75mM Tris-HCl pH 7.5, 6 mM EDTA), and 4 μ l of a mixture of mutant, wild-type, and gene-specific fluorescent probes, each at 5 μ M in TE buffer. The hybridization mixture was heated to 70°C for 10 s and slowly (0.1°C/s) cooled to 35°C. After incubating at 35°C for 2 min, the mixture was cooled (0.1°C/sec) to room temperature. The beads were collected with a magnet and the

supernatant containing the unbound probes was removed using a pipette. The beads were resuspended in 100 μ l of 1 \times hybridization buffer and heated to 48°C for 5 min to remove unbound probes. After the heating step, the beads were again separated magnetically and washed once with 100 μ l wash buffer. In the final step, the supernatant was removed and beads resuspended in 200 μ l TE buffer for flow cytometric analysis.

A LSR II flow cytometry system (BD Biosciences, Franklin Lakes, NJ) equipped with a high throughput autosampler was used for the analysis of each bead population. Beads with no extension product were excluded from the analysis.

Results

Twelve patients with resected metastatic colorectal cancer were enrolled in this study, accounting for a total of 12 resected tumors. All patients underwent major hepatic resection (> 3 segments) and had negative histologic margins (R0 resection). Ten patients had received chemotherapy at some point in their treatment prior to surgery, three of which had a measurable radiologic tumor response (minor response by RECIST criteria), and two were chemotherapy-naïve. On standard histologic assessment, all patients had evidence some residual tumor within the macroscopically evident metastasis.

The tumors within the liver were interrogated for a subset of mutations in APC, KRAS, PIK3CA and p53 by Sanger sequencing. Six tumors were found to have mutations of APC, four of KRAS, one of PIK3CA, and 1 of TP53, as shown in Table 1. These tumor-specific oncogenic mutations were used as markers to create probes (Supplementary Table 2) to detect the presence of tumor-specific mutant DNA in the liver tissue surrounding the tumor.

A total of 88 samples from the tumor periphery were probed for mutations present in the corresponding tumor using BEAMing. Punch biopsies of 4 mm in diameter were obtained in circumferential fashion around the macroscopically visible tumor-liver border, as shown in Figure 1 and Supplementary Figure 1.

Mutations identical with those identified in the tumor were detected outside of the visible tumor margin in only five of the 88 punch biopsies analyzed. All biopsies containing a mutation were detected only at the closest (4 mm) distance from the macroscopic tumor border, accounting for 20% (5/25) at the 4mm distance. None of the 63 samples at 8, 12 or 16 mm from the visible tumor margin contained tumor-specific mutant DNA (Table 1).

The biopsies with detectable tumor DNA beyond the histologic margin were only in patients who had received chemotherapy prior to surgery. Three of these four patients had an objective radiographic response to chemotherapy prior to surgery. The biopsies from the two chemotherapy-naïve patients did not have detectable DNA outside the tumor-normal border.

Margin status was confirmed independently in a blinded fashion by a pathologist who reviewed tissue from both ends of the punch biopsy cylinder using microscopic analysis. Malignant cells were noted in biopsies from four of the five punch biopsies with detectable mutant DNA (all at 4 mm). In these cases, nests of cancer cells could be observed in sections of tissue immediately adjacent to those used for genetic analyses. A representative case, where clusters of tumor cells were present, is shown in Supplementary Figure 2. In the fifth case with detectable mutant DNA, no tumor cells could be identified in such sections, even after extensive searching. Importantly, no tumor cells could be identified histopathologically in any of the 83 biopsies that did not contain mutant DNA.

Discussion

While mutations provide ideal tumor biomarkers, their use as a measure of minimal residual disease in pathologic specimens from solid tumor patients has been limited. One reason has been the much greater concentration of normal DNA at histologically normal tumor margins, making mutant DNA fragments difficult to detect with conventional technologies. In this study, we were able to overcome this limitation through the use of BEAMing.

There were two particularly notable results emanating from this study. First, 33% of tumors had evidence of tumor DNA beyond the macroscopically visible tumor-normal border but none had evidence of neoplastic cells or tumor DNA beyond 4 mm. These results support the clinical evidence that a negative (R0) margin may be sufficient. Second, we did not find evidence of residual tumor DNA in the region in which the tumor likely existed prior to chemotherapy, suggesting that tumors which respond to chemotherapy likely do so in a concentric fashion. In previous studies which have histologically investigated chemotherapy responses in patients with metastatic colorectal cancer to the liver, viable tumor was mostly found within the central region (10, 11). Similarly, Ng et al. reported, using standard histologic assessment, that most colorectal metastases contract centripetally when responding to chemotherapy (12).

Some qualification must be considered when interpreting these findings. One limitation is that our technical sensitivity is, conservatively, one tumor cell among 10,000 normal cells (6). We therefore would not be able to reliably detect tumor cell populations that were smaller than this. In addition, while the sampling was extensive, specimens of the peripheral tissue were still selective, allowing for the possibility of missed tumor extension, even using this highly sensitive methodology. Moreover, the overall number of patients in this study and number of patients with positive margins who received neo-adjuvant chemotherapy is comparatively small; further studies will be necessary to validate these findings. Finally, BEAMing cannot distinguish whether the mutant DNA arose from live tumor cells vs. dead ones left after chemotherapy. The accompanying histopathologic analysis overcame this limitation in most cases, as nests of cancer cells were detected in four of the five biopsies with mutant DNA. On the basis of morphologic criteria, these nests were very likely to be live cancer cells capable of progressive tumor growth.

In summary, our study provides additional evidence that normal negative histologic margin appears to be sufficient when resecting hepatic colorectal metastases, even following chemotherapy response. It will be informative to apply this same type of combined histopathologic-molecular analysis to other tumor types and locations.

Statement of Translational Relevance

How much normal tissue should be excised around a liver metastasis from a colorectal cancer? Determination of the margin status after surgical resection has major prognostic and therapeutic implications in patients with solid tumors. Assessment of the exact margin becomes more complex in the setting of preoperative chemotherapy that aims to decrease tumor size prior to resection. In this report, we utilize a digital PCR-based technique, termed BEAMing, which enumerates rare mutant DNA events in a pool of wild-type DNA. We applied this technique to measure rare mutant events in the tumor margins of liver metastases from colorectal cancer at varying distances from the tumor. The information obtained provides a scientific basis for determining the proper excisional margins and the approach we used can be generally applied to other tumor types and locations.

Supplementary Material

Refer to Web version on PubMed Central for supplementary material.

Acknowledgments

We thank for Lilian Dasko-Vincent in the microscopy core facility for technical assistance. This work was supported by the The Virginia and D. K. Ludwig Fund for Cancer Research, the Maryland Cigarette Restitution Fund and by the National Institutes of Health #CA129825 (LD). BV, LD and KWK are members of the Scientific Advisory Board of Inostics, a company that is developing technologies for the molecular diagnosis of cancer. BV, LD, and KWK also own stock in Inostics. BV, KWK and LD are members of the Scientific Advisory Board of PDGx and own stock in the company. The authors are entitled to a share of the royalties received by the University on sales of products related to genes described in this manuscript. The terms of these arrangements are being managed by the University in accordance with their conflict of interest policies. BV and KWK and Johns Hopkins University also own stock in Exact Sciences, which are managed under similar arrangements.

References

1. Choti MA, Sitzmann JV, Tiburi MF, Sumetchotimetha W, Rangsri R, Schulick RD, et al. Trends in long-term survival following liver resection for hepatic colorectal metastases. *Ann Surg*. 2002; 235(6):759–766. [PubMed: 12035031]
2. Muratore A, Ribero D, Zimmiti G, Mellano A, Langella S, Capussotti L. Resection margin and recurrence-free survival after liver resection of colorectal metastases. *Ann Surg Oncol*. 2010; 17(5): 1324–1329. [PubMed: 19847565]
3. Pawlik TM, Scoggins CR, Zorzi D, Abdalla EK, Andres A, Eng C, et al. Effect of surgical margin status on survival and site of recurrence after hepatic resection for colorectal metastases. *Ann Surg*. 2005; 241(5):715–722. discussion 722–4. [PubMed: 15849507]
4. Winter JM, Cameron JL, Campbell KA, Arnold MA, Chang DC, Coleman J, et al. 1423 pancreaticoduodenectomies for pancreatic cancer: A single-institution experience. *J Gastrointest Surg*. 2006; 10(9):1199–1210. discussion 1210–1. [PubMed: 17114007]
5. Diehl F, Li M, He Y, Kinzler KW, Vogelstein B, Dressman D. BEAMing: Single-molecule PCR on microparticles in water-in-oil emulsions. *Nat Methods*. 2006; 3(7):551–559. [PubMed: 16791214]
6. Li M, Diehl F, Dressman D, Vogelstein B, Kinzler KW. BEAMing up for detection and quantification of rare sequence variants. *Nat Methods*. 2006; 3(2):95–97. [PubMed: 16432518]
7. Rago C, Huso DL, Diehl F, Karim B, Liu G, Papadopoulos N, et al. Serial assessment of human tumor burdens in mice by the analysis of circulating DNA. *Cancer Res*. 2007; 67(19):9364–9370. [PubMed: 17909045]
8. Diehl F, Schmidt K, Choti MA, Romans K, Goodman S, Li M, et al. Circulating mutant DNA to assess tumor dynamics. *Nat Med*. 2008; 14(9):985–990. [PubMed: 18670422]
9. Jones S, Zhang X, Parsons DW, Lin JC, Leary RJ, Angenendt P, et al. Core signaling pathways in human pancreatic cancers revealed by global genomic analyses. *Science*. 2008; 321(5897):1801–1806. [PubMed: 18772397]
10. Benoist S, Brouquet A, Penna C, Julie C, El Hajjam M, Chagnon S, et al. Complete response of colorectal liver metastases after chemotherapy: Does it mean cure? *J Clin Oncol*. 2006; 24(24): 3939–3945. [PubMed: 16921046]
11. Adam R, Wicherts DA, de Haas RJ, Aloia T, Levi F, Paule B, et al. Complete pathologic response after preoperative chemotherapy for colorectal liver metastases: Myth or reality? *J Clin Oncol*. 2008; 26(10):1635–1641. [PubMed: 18375892]
12. Ng JK, Urbanski SJ, Mangat N, McKay A, Sutherland FR, Dixon E, et al. Colorectal liver metastases contract centripetally with a response to chemotherapy: A histomorphologic study. *Cancer*. 2008; 112(2):362–371. [PubMed: 18041069]

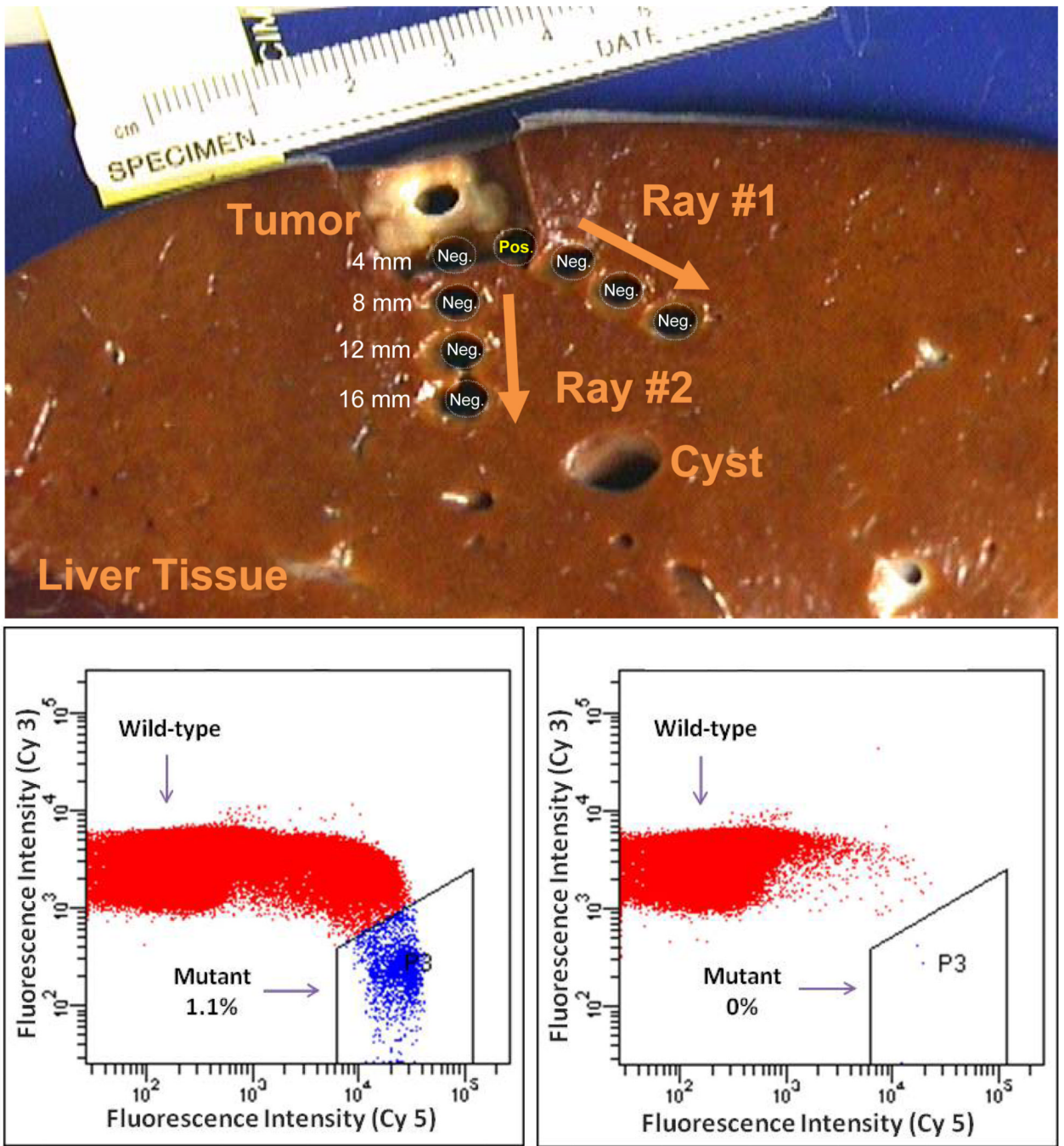


Figure 1. Detection of tumor-specific mutated DNA in the margin surrounding a colorectal cancer liver metastasis

Punch biopsies were obtained at 4 mm distances from the macroscopically visual tumor margin. Shown below are flow cytometric data from BEAMing reactions of a sample at 4 mm that was macroscopically normal appearing but with detectable mutant DNA (left) and a sample at 8 mm distance from the same lesion that did not show presence of mutated tumor DNA (right).

Table 1

Patient Characteristics and Molecular Margin Status.

Patient No.	Age	Gender	Chemotherapy	Response	Gene	Exon	Mutation	Ray	Fraction mutated, wild type DNA; distance from tumor (mm)				Histopathology; distance from tumor (mm)					
									4	8	12	16	4	8	12	16		
1	51	M	Yes (neo)	Yes	APC	5	C637T	A	<u>1.09</u>	ND	ND	ND	ND	<u>Pos</u>	Neg	Neg	Neg	Neg
								B	ND	ND	ND	ND	ND	Neg	Neg	Neg	Neg	Neg
								A	<u>0.22</u>	ND	-	-	-	<u>Pos</u>	Neg	-	-	-
2	47	M	Yes (neo)	Yes	APC	15	C4012T	B	ND	ND	-	-	-	Neg	Neg	-	-	-
								C	ND	ND	ND	-	-	Neg	Neg	Neg	-	-
								D	ND	-	-	-	-	Neg	-	-	-	-
3	55	M	Yes (neo)	Yes	KRAS	1	G35A	A	<u>0.97</u>	ND	ND	-	-	<u>Pos</u>	Neg	-	-	-
								B	<u>0.92</u>	ND	ND	ND	ND	<u>Pos</u>	Neg	Neg	Neg	Neg
4	59	F	Yes (neo)	Yes	TP53	8	C844T	A	ND	ND	ND	ND	ND	Neg	Neg	Neg	Neg	Neg
								B	ND	ND	-	-	-	Neg	Neg	-	-	-
5	52	F	Yes (neo)	Yes	KRAS	1	G35T	A	ND	ND	ND	ND	ND	Neg	Neg	Neg	Neg	Neg
								B	ND	ND	ND	ND	ND	Neg	Neg	Neg	Neg	Neg
6	41	F	Yes (neo)	Stable	APC	6	C646T	A	ND	ND	ND	ND	ND	Neg	Neg	Neg	Neg	Neg
								B	ND	ND	ND	ND	ND	Neg	Neg	Neg	Neg	Neg
7	63	M	Yes (adj)	N/A	PIK3CA	20	A3140G	A	ND	ND	ND	ND	ND	Neg	Neg	Neg	Neg	Neg
								B	ND	ND	ND	ND	ND	Neg	Neg	Neg	Neg	Neg
8	69	M	Yes (adj)	N/A	KRAS	1	G35A	A	ND	ND	ND	ND	ND	Neg	Neg	Neg	Neg	Neg
								B	ND	ND	ND	ND	ND	Neg	Neg	Neg	Neg	Neg
9	64	F	Yes (adj)	N/A	KRAS	1	G35C	A	ND	ND	ND	ND	ND	Neg	Neg	Neg	Neg	Neg
								B	ND	ND	ND	ND	ND	Neg	Neg	Neg	Neg	Neg
10	53	M	Yes (neo)	Stable	APC	15	4165del TC	A	ND	ND	ND	ND	ND	Neg	Neg	Neg	Neg	Neg
								B	<u>0.07</u>	ND	ND	ND	ND	Neg	Neg	Neg	Neg	Neg
11	74	M	No	N/A	APC	15	4241-4242 ins T	A	ND	ND	ND	ND	ND	Neg	Neg	Neg	Neg	Neg
								B	ND	ND	ND	ND	ND	Neg	Neg	Neg	Neg	Neg
12	74	M	No	N/A	APC	15	3927del AAAGA	A	ND	ND	ND	ND	ND	Neg	Neg	Neg	Neg	Neg
								B	ND	ND	ND	ND	ND	Neg	Neg	Neg	Neg	Neg

neo - neoadjuvant chemotherapy
adj - prior adjuvant chemotherapy

samples positive for mutation are outlined
ND - No mutant DNA detected
Neg - Negative